Solar Irradiance Prediction using Deep Learning

Yassir El Mesbahi, Raghav Gupta, Bhavya Patwa, Sabi Traifi
Department of Computer Science and Operations Research
University of Montreal, Quebec, Canada

1 Introduction

Climate change is one of the most pressing issues of the 21^{st} century. Renewable energy sources such as solar and wind power provide a clean alternative to fossil fuels and their devastating CO2 emissions. However, integrating such sources of energy into the electricity grid requires accurate predictions to maintain supply-demand adequacy and this is a difficult task due the uncertainty and variability of wind and solar resources (14).

Recent advances in machine learning can certainly play a role in tackling climate change (5). In this project, we focus on solar energy and explore deep learning techniques for Global Horizontal Irradiance (GHI) nowcasting. GHI, expressed in Watt per square meter (W/m^2), measures the amount of solar irradiance falling on a horizontal surface on earth, and has a direct impact on solar power generation. It is therefore crucial to have reliable GHI predictions.

We use geostationary satellite images to predict present and future GHI values within a 6-hour horizon: given satellite images up to time T_0, we aim to predict GHI values at T_0, $T_0 + 1h$, $T_0 + 3h$ and $T_0 + 6h$. Solar irradiance depends on several factors such location, elevation, time of the day and weather conditions, most notably *cloudiness*.

Our data consists of GHI values measured at seven distinct SURFRAD ground stations in the USA, together with GOES13 satellite images of the USA from April 2010 to December 2015, capturing atmospheric properties at different wavelengths (5 channels). The data is available at 15-minute intervals, with some missing data (missing images and/or GHI values) . For the sake of generalization, we aim at predicting GHI values using only satellite images, as opposed to less flexible GHI time-series approaches.

The *Clear-Sky model* provides an empirical estimation for the GHI value in "clear sky" (i.e. cloud-free) conditions at any point on earth, given a latitude, longitude, elevation, date and time (13). Our data also includes the clear-sky GHI values computed at each 15-minute timestamp for each station, as well as a discrete measure of "cloudiness" derived heuristically from the observed GHI values and the clear-sky GHI estimates ("clear", "cloudy", "slightly cloudy", "variable") (6).

Current GHI prediction models that use satellite (or ground-based) images rely mostly on extrapolation of cloud motion (and more precisely horizontal cloud advection) to derive a cloud-index factor, which is then combined with a clear-sky model to estimate GHI values (15). In this paper, we show that deep learning techniques such as Convolutional Neural Network models can be used to predict GHI values accurately using satellite images.

Because estimating present and future GHI values is a regression task, we use *Root Mean Square Error (RMSE)* to assess the performance of GHI predictions with our deep learning models. We compare our results against the naive clear-sky model.

The next chapters are organized as follows: *section 2* covers the literature review, *section 3* provides analysis of the data, *section 4* outlines our methodology and the models we used, and *section 5* discusses our results. Finally, in *section 6*, we list our conclusions and provide directions for future work. We assume the reader to be knowledgeable about machine learning and deep learning.

2 Literature Review

There exists a large literature describing various techniques for irradiance forecasting. Many of these forecast GHI values based on time series of past GHI ground measurements. This need for ground measurements severely limits the actual use of such methods, as they cannot generalize to locations for which ground measurements are not available.
In this paper, we focus on techniques that predict irradiance based on satellite images. Because the irradiance is directly influenced by the weather and cloudiness, it is also worth looking at image-based weather forecast models, especially those predicting cloud motion. In this section, we discuss existing image-based techniques that forecast irradiance and precipitation. We then cover recent attempts at using deep learning for such tasks, as well as other deep learning models that seem promising for irradiance prediction.

2.1 Satellite cloud motion vectors

Existing intra-day GHI forecast models often rely on cloud motion vectors derived from consecutive satellite images to predict future images. Using the semi-empirical Heliosat method (7), a cloud index is computed for each pixel and then applied to a clear-sky model to derive GHI predictions. This is summarized in the diagram below (**?**):

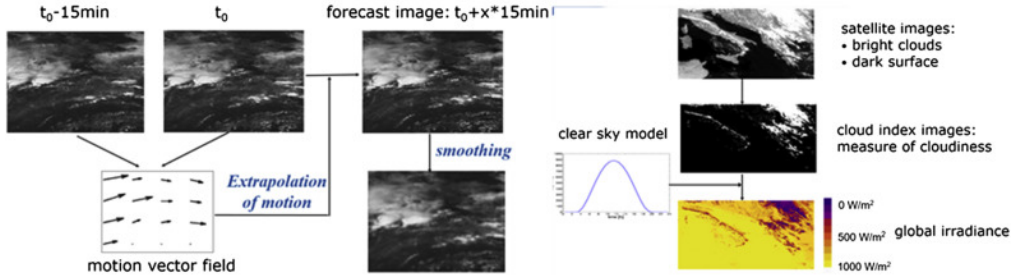

Fig. 1: Flowchart of GHI prediction

Although the origins of this method can be traced back several decades ago (for example (2)), its principles are still applied in recent studies on satellite-based irradiance forecasting, such as (20).

With deep learning techniques, we would like to build similar models, which learn to predict irradiance accurately given sequences of satellite images, but without the need for "human-engineered" empirical formulas.

2.2 Precipitation forecasting using deep learning

Cloud motion prediction is also key to forecast rainfall, and therefore it is interesting to study recent deep learning techniques applied to precipitation forecasting.
Recently, Google described a precipitation nowcasting model using radar images (1). Based on the *U-Net* convolutional neural network (CNN) (16), the model infers the meteorological evolution from a sequence of input images, without incorporating atmospheric data into the model. The U-Net model consists of an encoding phase made of a sequence of layers that successively decrease the resolution of the images, followed by a decoding phase that reconstructs the initial image from the low-dimensional representations. It was initially designed for biomedical image segmentation.
For short forecast horizons (up to 4 hours), this model outperforms Optical Flow, Persistence and even the High-Resolution Rapid Refresh (HRRR) forecast model used by the US National Oceanic and Atmospheric Administration (11). A similar architecture for precipitation nowcasting using satellite images is described in (10).

Another interesting deep learning approach to precipitation nowcasting is the use of a "Convolutional Long-Short Term Memory (LSTM)" network (17), as well as the improved "Trajectory Gated Recurrent Unit (GRU)" model that was later proposed by the same authors (18). These models successfully implement spatio-temporal sequence forecasting, using an encoding-forecasting structure.

2.3 Irradiance forecasting using Deep Learning

Solar irradiance nowcasting based on images is still an active area of research. Recently, a few studies have proposed deep learning models irradiance forecasting using *sky imaging*. We summarize below some of the proposed solutions:

- **3D-CNN** (21): provides a simple 3D-CNN model for very-short-term irradiance prediction.
- **CNN+LSTM** (19): process sequences of video frames from sky imaging, together with auxiliary weather data, to forecast irradiance up to 4 hours ahead, using CNN and LSTM networks.
- **SolarNet** (3): proposes a deep CNN (inspired by VGG16 (9)) to predict short-term (10 minutes ahead) GHI values.
- **KloudNet** (4): uses a ResNet architecture (8) to predict a very-short-term "cloudiness" state (classification).

As expected, most models in the literature use the CNN architecture, at this is well suited for computer vision tasks.

3 Data Analysis

3.1 Types of data

The data origins from two sources - the GOES 13 satellite and the SURFRAD data. The SURFRAD data provides information about the coordinates(latitude, longitude, elevation) of the seven stations where measures are made. The GOES 13 satellite data consists in satellite images, Clearsky GHI values(floats), ground truth GHIs(floats), cloudiness(categorical), daytime(categorical) and timestamps(when images have been recorded). Each image comes with 5 channels:

- Red (visible spectrum)
- Infrared (smaller wavelengths)
- Infrared (water vapour)
- Infrared (bigger wavelengths)
- Infrared (CO_2)

The figure below shows sequences of images with 15 minutes interval:

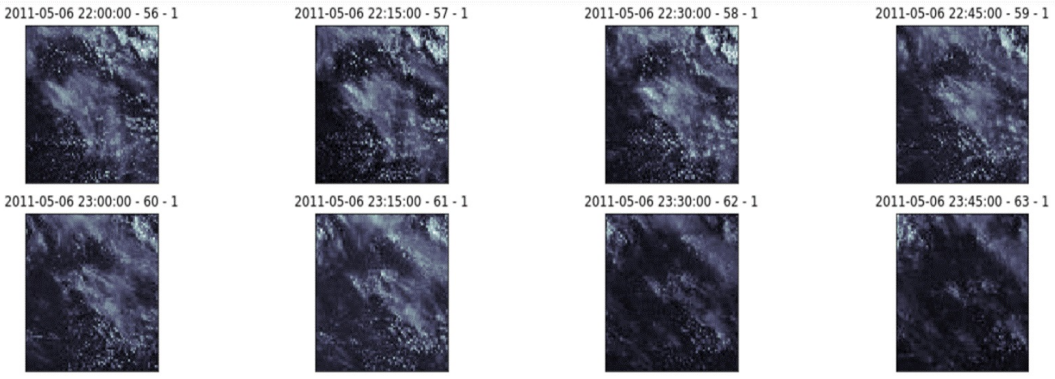

Fig. 2: Sequences of images

Also, it should be noted that images come in three different formats: net cdf files (high resolution, one file per 15 minutes) and compressed 16-bit and 8-bit hdf5 files(lesser resolution, one file per day).

The figure below shows the distribution of the GHIs with respect to the stations:

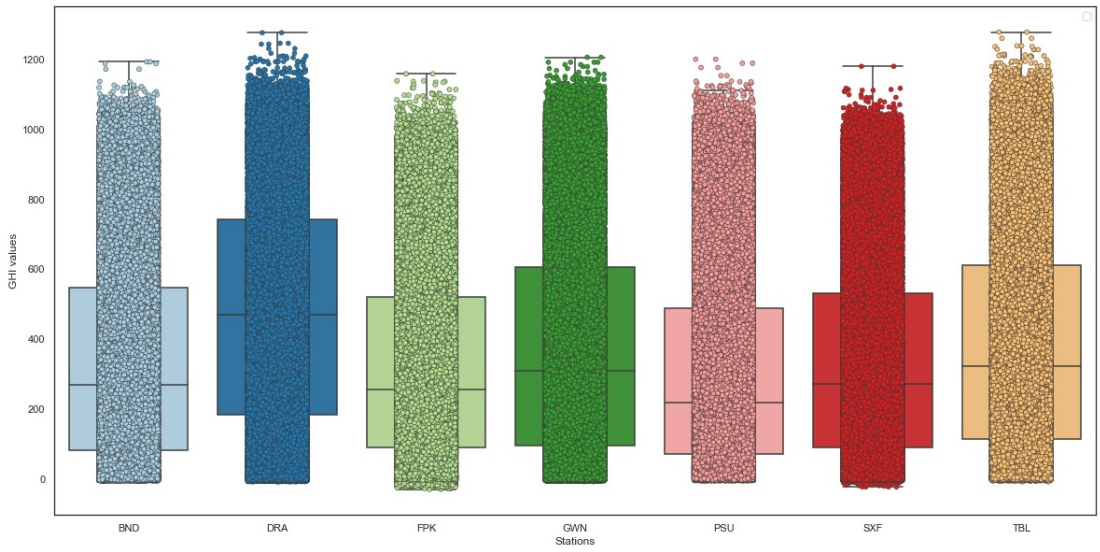

Fig. 3: Distribution of the GHI values per station

At last but not least, all the above data, along with the paths to images are provided in pandas data frame containing 210336 rows, separated by 15-minute intervals starting from 2010 and ending at 2015, which represents 2192 days in total.

3.2 Missingness of data

The data is not thoroughly clean and requires pre-processing. Around 17.4% of the data does not have an image associated with it. The figure below describes the percentages of missing images per year:

2010	2011	2012	2013	2014	2015
37.21%	12.69%	17.75%	15.81%	10.50%	10.49%

Table 1: Percentages of missing data per year

Clearsky and ground truth GHIs are also missing, as shown in the table below:

BND	TBL	DRA	FPK	GWN	PSU	SXF
180	514	1258	567	2575	228	763

Table 2: Numbers of missing GHIs per station

We also notice that some channels are corrupted, as shown in the image below:

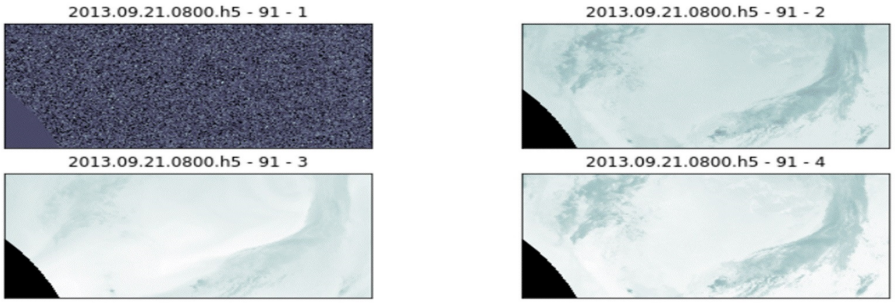

Fig. 4: Unavailability of the first channel for a sample (only four channels shown)

3.3 Some preliminary tests

In order to have an idea of how good should our models perform, we have decided to run small tests to check the performance of the clear-sky model. The table below describes the results we obtained for T_0 and $T_0 : T_0 + 4$:

Dataset	MSE error	RMSE error
Train	41300.81	203.23
Valid	44895.35	211.88

Table 3: Clearsky model performance on T_0 predictions

4 Methodology

The sub-sections describe design decisions and the data pipeline we implemented.

4.1 Data pre-processing

We first fill the clear-sky GHIs and in situ GHIs which are *Not-a-Number (NaN)* with 0 if *daytime* is 0, that is, if it is night. Then for dealing with NaNs GHI and Clear-sky GHI in daytime, we linearly interpolate data. Although these interpolated values do go into validation set as well, we argue that the NaNs are very less compared to the entire dataset $[000\%]$. Negative GHI values are set to 0.

4.2 Data Split

We do a train-validation- test split of 79%-20%-1% on the catalog dataframe, which amounts to 1605 days, 416 days, 26 days respectively. The year 2015 represents most of our validation dataset and we keep 1% as a sanity-check dataset. We shuffle the rows of the training set as this would create batches with different seasons and weather conditions, hence discouraging the model from learning on just one season or weather condition.

4.3 Sequences generation

We iterate over each row (15 minute data), calculate the sequences timeframes, looking back in time for images and looking ahead in time for clear-sky and ground measurement GHIs. We observed that a time interval of 30 minutes between two images in a sequence is the right balance to allow capturing cloud movement in crops of reasonable size. We chose the number of sequences to be 3, including T_0, for computation purposes.

4.4 Image crops

We extract each station's crops with a crop size of 70x70 pixels, which amounts to 280 km^2. We standardize the crops across channels using the mean and standard deviation calculated beforehand on the training dataset. Rather than outputting the forecasted GHI value, We make the model learn the difference between the clear-sky GHIs and actual GHIs. We hypothesize that the model can be a better version of the clear-sky model, by not just learning the prior assumptions from the clear-sky model, but also from the infrared channels of the satellite images.

4.5 Meta-data

Meta-data is extracted from the *iso-datetime* index of the catalog provided. We extract the features of day, month and time represented in ranges $1-31$, $1-12$ and $0-23$ ranges respectively. We need to extract meaningful representation out of these values as there can be a relation like seasons in months, GHI variation according to time, etc. Hence, we would like to represent these features where similar values are together and hence this leads to formations of distinct latent groups.

There are hand feature engineering techniques like taking cos and sin of time to get circular transformed features (12), but we harbour the power of back-propagation to find the latent patterns in these variables. One way of achieving this desired result is by creating a lookup table with each value of a variable corresponding to some randomly initialized vector. These values are replaced by their vector during forward propagation and the vectors are updated during back-propagation using

gradients. We choose vector lengths of 4, 5 and 4 for day, month and time respectively.

We do not use the latitude or longitude or elevation as input to the model, because these are distinctly identifiable values of their corresponding stations and we suspect that the model might train to act like 7 “sub-models”, hence not generalizing to any point on the satellite map. Although we could remove the "channel 1" noisy examples by identifying them through a histogram-based method, we decided to keep them to use this noise as regularization. In any case, we observed that most of these irregularities occur at night time.

4.6 Models

In terms of models, we have implemented the 2D-CNN and 3D-CNN, and tested the performance of both with meta-data and without meta-data.
When also using meta-data as input, we make use of a multi-modal architecture to train the network both with meta-data and images. Image goes through the CNN network and meta-data through fully connected layers. We then concatenate both into a single vector, pass it through a fully connected layer before the final output fully connected layer.

The loss used to train the model is the mean square error and the validation is the RMSE.

the 3D-CNN Model Architecture with Metadata is described below:

4.7 Hyper-parameter tuning

The hyper-parameters that gave the best results are:

- Number of Epochs: 10
- Optimizer: Adam
- Learning Rate: 0.001
- Image Crop Size: 70*70
- Image Sequence Size: 3
- Offset between 2 images in the sequence: 30 minutes

We did not use data augmentation techniques in the project as the size of our training set was already significant.

5 Results

The table below provides the training and validation RMSE scores observed on the 3 models we trained:

Model	Train RMSE	Validation RMSE
2D-CNN no metadata	100	119
3D-CNN no metadata	114	168
3D-CNN with metadata	116	120

5.1 Discussion

Quite surprisingly, the best model we trained was the 2D-CNN without meta-data, with a validation RMSE at 119 W/m^2, almost similar to the 120 W/m^2 validation RMSE of the 3D-CNN with meta-data. We were expecting 3D-CNN to learn from image sequences much more than the 2D-CNN.

Adding meta-data to the 3D-CNN model brought a significant improvement to the model’s performance.

Our models performed better than the naive clear sky model (whose RMSE is 210 for T_0 prediction and 190 for the further GHI values).

5.2 Why is it hard to predict solar irradiance several hours ahead in the future?

Solar radiations reaching earth surface depend in most part of the clearness of the sky (i.e. clouds may considerably reduce the amount of solar irradiance passing through). Therefore, due to the unexpectedness of the winds, some clouds may non-deterministically hide the sun lights for some times in the day, thus causing drops in the measured GHIs. The figure below shows both of the diagrams of clearsky GHI and actual GHI measured during a day when a cloud passes by:

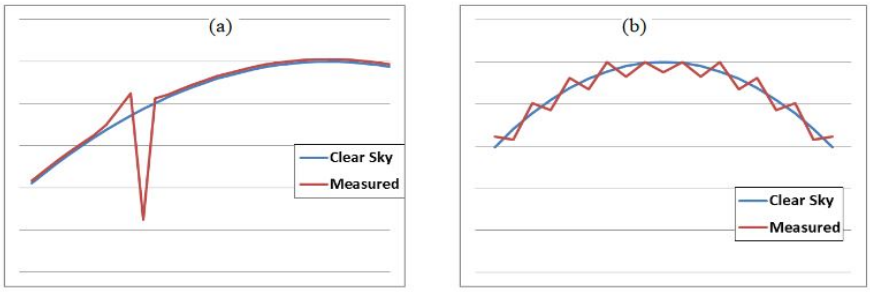

Fig. 5: Influence of the clouds on the actual GHI

We can see a dramatic change in the curve in figure (a), which explains why sometimes the measures suddenly drop to very low values even when at daytime.

6 Conclusions and future work

6.1 Conclusion

As a conclusion, we do believe that the results we have obtained using the previously-mentioned models gave decent results, considering the difficulty of the task. As we have explained before, several non-deterministic factors (in particular weather changes) can greatly impact the GHI measures and thus degrade models performances. Moreover, the noise induced by the missingness in the data (missing images/channels, missing GHIs, ...) had also a noxious effect on the performance of our models.

6.2 Recommendation for future work

If we had more time, we could have tested models that include recurrent structures, such as the Trajectory GRU model described in the literature review above. Moreover, introducing attention mechanisms probably help the model focus at the center of the image crop.

Some of our tests that ran on numerical data only (including the cloudiness factor) have outperformed the models using images (RMSEs between 40 and 60), which leads us to the conclusion that a future improvement of our models would be to use sequences of images to predict the cloudiness factor only (floating value between 0 and 1), and use the predictions of the model with other numerical data (that could be obtained by simple calculations) to infer future GHIs.

Bibliography

[1] AGRAWAL, S., ET AL. Machine learning for precipitation nowcasting from radar images.

[2] CANO, D., ET AL. A method for the determination of the global solar radiation from meteorological satellites data.

[3] CONG FENG, J. Z. Solarnet: A deep convolutional neural network for solar forecasting via sky images.

[4] ET AL., D. P. Kloudnet: Deep learning for sky image analysis and irradiance forecasting.

[5] ET AL., D. R. Tackling climate change with machine learning.

[6] G.M. TINAA, S. DE FIOREM, C. V. Analysis of forecast errors for irradiance on the horizontal plane.

[7] HAMMER, A., ET AL. Solar energy assessment using remote sensing technologies.

[8] KAIMING HE, XIANGYU ZHANG, S. R. J. S. Deep residual learning for image recognition.

[9] KAREN SIMONYAN, A. Z. Very deep convolutional networks for large-scale image recognition.

[10] LEBEDEV, V., ET AL. Precipitation nowcasting with satellite imagery.

[11] LEBEDEV, V., ET AL. Using machine learning to "nowcast" precipitation in high resolution. google research.

[12] LONDON, I. Blogpost: encoding cyclical continuous features - 24-hour time.

[13] MATTHEW J. RENO, CLIFFORD W. HANSEN, J. S. S. Global horizontal irradiance clear sky models: Implementation and analysis.

[14] NOTTON, G., AND VOYANT, C. Forecasting of intermittent solar energy resource. in advances in renewable energies and power technologies, volume 1, chapter 3: Solar and wind energies (pages 77-114).

[15] PHILIPPE BLANC, JAN REMUND, L. V. Short term solar power forecasting based on satellite images.

[16] RONNEBERGER, O., ET AL. U-net: Convolutional networks for biomedical image segmentation.

[17] SHI, X., ET AL. Convolutional lstm network: A machine learning approach for precipitation nowcasting.

[18] SHI, X., ET AL. Deep learning for precipitation nowcasting: A benchmark and a new model.

[19] SIDDIQUI, T. A., ET AL. A deep learning approach to solar-irradiance forecasting in sky-videos.

[20] VIIVI KALLIO-MYERS, AKU RIIHELÄ, P. L. A. L. Global horizontal irradiance forecast for finland based on geostationary weather satellite data.

[21] ZHAO, X., ET AL. 3d-cnn-based feature extraction of ground-based cloud images for direct normal irradiance prediction.